HHS Public Access

Author manuscript

Hippocampus. Author manuscript; available in PMC 2017 August 01.

Published in final edited form as:

Hippocampus. 2016 August ; 26(8): 980–994. doi:10.1002/hipo.22580.

Synergistic stress exacerbation in hippocampal neurons: Evidence favoring the dual hit hypothesis of neurodegeneration

Scott D. Heinemann[1,^], **Jessica M. Posimo**[1,^], **Daniel M. Mason**[1], **Daniel F. Hutchison**[1], and **Rehana K. Leak**[1,*]

[1]Division of Pharmaceutical Sciences, Duquesne University, Pittsburgh PA

Abstract

The dual hit hypothesis of neurodegeneration states that severe stress sensitizes vulnerable cells to subsequent challenges so that the two hits are synergistic in their toxic effects. Although the hippocampus is vulnerable to a number of neurodegenerative disorders, there are no models of synergistic cell death in hippocampal neurons in response to combined proteotoxic and oxidative stressors, the two major characteristics of these diseases. Therefore, we developed a relatively high-throughput dual hit model of stress synergy in primary hippocampal neurons. In order to increase the rigor of our study and strengthen our interpretations, we employed three independent, unbiased viability assays at multiple timepoints. Stress synergy was elicited when hippocampal neurons were treated with the proteasome inhibitor MG132 followed by exposure to the oxidative toxicant paraquat, but only after 48h. MG132 and paraquat only elicited additive effects 24h after the final hit and even loss of heat shock protein 70 activity and glutathione did not promote stress synergy at this early timepoint. Dual hits of MG132 elicited modest glutathione loss and slightly synergistic toxic effects 48h after the second hit, but only at some concentrations and only according to two viability assays (metabolic fitness and cytoskeletal integrity). The thiol N-acetyl cysteine protected hippocampal neurons against dual MG132/MG132 hits but not dual MG132/paraquat hits. Our findings support the view that proteotoxic and oxidative stress propel and propagate each other in hippocampal neurons, leading to synergistically toxic effects, but not as the default response and only after a delay. The neuronal stress synergy observed here lies in contrast to astrocytic responses to dual hits, because astrocytes that survive severe proteotoxic stress resist additional cell loss following second hits. In conclusion, we present a new model of hippocampal vulnerability in which to test therapies, because neuroprotective treatments that are effective against severe, synergistic stress are more likely to succeed in the clinic.

Keywords

Parkinson’s disease; Alzheimer’s disease; N-acetylcysteine; dual-hit; two-hit; two hit; dual hit

*For correspondence, please address: Rehana K. Leak, Ph.D., Division of Pharmaceutical Sciences, Duquesne University, 600 Forbes Ave, Pittsburgh PA 15282, TEL: 412.396.4734, FAX: 412.396.4660, leakr@duq.edu.

^these authors did equivalent work

None of the authors have any conflicts to disclose.

Introduction

The hippocampus is highly vulnerable to pathology in disorders such as Alzheimer's disease, leading to severe cognitive impairments (Braak and Braak, 1995; Raskin et al., 2015). Studies in stroke victims further support the view that loss of neurons in this structure leads to cognitive dysfunction (Nikonenko et al., 2009). The hippocampus is also vulnerable to psychosocial and physical restraint-induced stress (McEwen and Magarinos, 1997), to epileptic seizure activity (Depaulis and Hamelin, 2015; Toth and Magloczky, 2014) and to atrophy in late stages of Parkinson's disease (Camicioli et al., 2003; Kandiah et al., 2014; Xia et al., 2013). Bruce McEwen hypothesized that the initial response to stress in the hippocampus is adaptive, but that this progresses into damage if the stress is chronic and unremitting (McEwen, 2001), consistent with Hans Selye's original dualistic view of stress (Selye, 1975). Heiko Braak observed that the phylogenetically ancient allocortex, of which the hippocampus is a major component, is more vulnerable to tau and alpha-synuclein pathology in Alzheimer's and Parkinson's disease than the neighboring neocortex (Braak and Braak, 1995; Braak et al., 2003; Braak et al., 2000b). We recently confirmed that neurons from the sensorimotor neocortex are less vulnerable to proteotoxic stress than neurons from three subregions of allocortex: hippocampus, entorhinal cortex, and piriform cortex (Posimo et al., 2013; Posimo et al., 2015). Cellular stress from loss of protein homeostasis combined with redox imbalance is a major hallmark of neurodegenerative disorders (Blesa et al., 2015; Jucker and Walker, 2013; Kim et al., 2015; Walker et al., 2006; Wang et al., 2014). Thus, as a major component of the allocortex, it is important to develop robust models of combined proteotoxic and oxidative stress in the hippocampus and to identify therapies that can mitigate severe injury in neurons from this vulnerable brain region.

In the present study, we developed a unique model of severe hippocampal stress in which to test new therapies. Our studies are based on the assumption that stress vulnerability and stress tolerance can be quantified by exposing previously stressed cells to a second stressful challenge and subsequently measuring viability (Leak, 2014). If the dual hits are synergistic in their toxic effects, the first exposure is hypothesized to sensitize cells to the second hit. This phenomenon of stress exacerbation is known as the dual hit or two hit hypothesis of neurodegeneration (Carvey et al., 2006; Leak, 2014). Many authors have applied the dual hit hypothesis to the hippocampus, in terms of epilectic seizure activity, schizophrenia, temporal sclerosis, memory loss, and Alzheimer's disease (Dalton et al., 2012; Hamelin and Depaulis, 2015; Hill et al., 2014; Hoffmann et al., 2004; Lewis, 2005; Llorente et al., 2011; McCarley et al., 1999; Ouardouz et al., 2010; Somera-Molina et al., 2007; Zhu et al., 2007). However, there is no model of synergistic cell death in hippocampal neurons in response to sequential hits of proteotoxic and oxidative stressors, the two major features of neurodegenerative disorders. The present study was therefore founded upon two overarching hypotheses. First, we speculate that proteotoxic and oxidative stressors amplify one another, so that exposures to high levels of both injuries synergize and then potentiate cell loss, culminating in neurodegenerative conditions. Second, we hypothesize that exposure to severe oxidative or proteotoxic stress also exacerbates the response to subsequent exposures to the same type of

insult, because endogenous defenses handling that specific type of injury are readily depleted by the first hit in vulnerable types of neurons.

In contrast to synergistic stress exacerbation, if two hits are only additive in their toxic effects, then the first hit is not hypothesized to have any impact on the response to the second hit (Leak, 2014). Alternatively, if the first hit blocks the toxic response to the second exposure, the cells have developed tolerance and are preconditioned against further challenges, as reported in primary astrocytes and dopaminergic cells (Gleixner et al., 2015; Leak et al., 2006; Leak et al., 2008; Titler et al., 2013). In the primary astrocyte studies, the cells that managed to survive an initial proteotoxic hit tolerated subsequent insults better than stress-naïve astrocytes and continued to protect neighboring primary neurons in neuron/glia co-cultures, suggesting that some cells can be preconditioned even by high-dose toxic stimuli and continue to fulfill their evolutionary roles. In the glial injury model, the first proteotoxic hit elicited a robust increase in glutathione whereas inhibition of glutathione defenses unmasked the underlying vulnerability to the second hit, rendering previously stressed astrocytes highly sensitive to subsequent stress exposures. In contrast to the astrocyte studies, neuroblastoma cells were sensitized to second proteotoxic or oxidative challenges when first exposed to toxic concentrations of the same insults, consistent with the dual hit hypothesis of neurodegeneration (Unnithan et al., 2012; Unnithan et al., 2014). In the neuroblastoma model, dual hits elicited severe loss of glutathione whereas the thiol N-acetyl cysteine (NAC) mitigated the loss in glutathione and abolished the synergistic response to dual hits. These findings suggest that stress resilience or vulnerability is determined by up- or downregulation of glutathione levels, respectively.

Based on the results of our previous studies and the known vulnerability of the hippocampus to multiple disease states, here we attempted to develop a dual hit model of severe stress in primary hippocampal neurons, measured glutathione levels, and examined the therapeutic potential of NAC against severe injury. The herbicide paraquat was used to generate oxidative stress, and the proteasome inhibitor MG132 was used to model proteotoxic stress. Paraquat exposure is a risk factor for Parkinson's disease and has been used by many investigators to model this condition in animals (Blesa et al., 2012; Jones et al., 2014; Tanner et al., 2011). Oral paraquat administration has been shown to reduce ATP generation and increase oxidative stress in the hippocampus *in vivo*, and to elicit neurological impairments in the Morris water maze test, a behavioral assay closely associated with hippocampal integrity (Chen et al., 2010). Indeed, the hippocampus is especially sensitive to complex 1 inhibition and mitochondrial dysfunction (Navarro and Boveris, 2010; Navarro et al., 2008), the proposed mechanism of action of paraquat (Cocheme and Murphy, 2008). As a model of proteotoxic stress, we applied the peptide aldehyde MG132, which is commonly used to prevent the degradation of misfolded proteins through the proteasome particle (Lee and Goldberg, 1998). Proteasome inhibition increases the burden of misfolded, aggregated proteins and elicits neurodegeneration (Rideout et al., 2001; Rideout and Stefanis, 2002; Sun et al., 2006). Modeling loss of proteasome function is clinically relevant because Parkinson's and Alzheimer's disease are both characterized by inhibition of proteasome activity in brain tissue (Keller et al., 2000a; McNaught et al., 2002; McNaught and Jenner, 2001). Furthermore, Parkinson's and Alzheimer's disease both involve dense protein aggregations (Braak and Braak, 1995; Braak et al., 1993; Braak et al., 2000a; Braak et al., 2002; Braak et

al., 2003; Braak et al., 2000b). For example, the hippocampus exhibits tau aggregations in Alzheimer's disease and alpha-synuclein aggregations in the CA2/CA3 subfields in Parkinson's disease (Bertrand et al., 2004; Beyer et al., 2013; Braak and Braak, 1995; Braak and Braak, 1997a; Braak and Braak, 1997b; Braak et al., 2003). Finally, Alzheimer's and Parkinson's disease involve atrophy and/or cell loss in the hippocampus (Gomez-Isla et al., 1997; Kalaitzakis et al., 2009; Schroder and Pantel, 2016).

The results of the present study demonstrate that severely stressed hippocampal neurons are sensitized to subsequent challenges according to three independent and unbiased viability assays, but only in a delayed manner and only with some treatment protocols. Thus, stress synergy is not the default consequence of dual hits but is dependent upon the cellular context. NAC was able to protect against proteotoxic but not oxidative stress in our model. In sum, we have presented a new model of synergistic stress exacerbation in hippocampal neurons for the rigorous testing of potential therapies.

Methods

Primary Cultures and Treatments

Tissue from the hippocampus was harvested from Sprague Dawley rat brains on postnatal day 1 or 2 (Charles River, Wilmington, MA). Tissue chunks were dissociated and plated as previously described in Neurobasal-A media with the supplement B27 (Crum et al., 2015; Posimo et al., 2015). Cultures were treated with MG132 (EMD Millipore, Billerica, MA) or paraquat (Sigma-Aldrich, St. Louis, MO) on day *in vitro* 5 (DIV5) for 24h. This was referred to as the 1st hit and was added to the existing media as a 10× solution. On DIV6, media were completely removed and cultures were treated with fresh MG132 or paraquat in a 1× solution. This DIV6 protocol facilitated the complete removal of the 1st hit and was referred to as the 2nd hit. Twenty-four or 48h later, on DIV7 or DIV8, cell viability was measured as described below. Wherever indicated, the heat shock protein 70 / heat shock cognate 70 (Hsp70/Hsc70) inhibitor VER155008 (R&D Systems, Minneapolis, MN; Massey et al., 2010; Schlecht et al., 2013) or the glutathione synthesis inhibitor buthionine sulfoximine (Griffith, 1982) was applied concurrently with MG132 and paraquat.

Viability Assays

Viability was measured using immunocytochemistry for the specific neuronal marker microtubule associated protein 2 (MAP2) with the infrared In-Cell Western technique, as published (Posimo et al., 2013; Posimo et al., 2014). Glutathione levels were measured in the same manner, according to published protocols (Posimo et al., 2013; Titler et al., 2013; Unnithan et al., 2012). Primary antibodies are listed in Supplemental Table S1. Infrared secondary antibodies were then applied to visualize MAP2 or glutathione (LI-COR Bioscience, Lincoln, NE; Jackson Immunoresearch Laboratories, Bar Harbor, ME). Immunolabeled cultures were also stained with the infrared nuclear stain DRAQ5 (1:10,000; Biostatus, Shepshed, Leicestershire, UK) for the second viability assay. All infrared staining was analyzed on an Odyssey Imager (Version 3.0, LI-COR Bioscience). As a third viability measure, levels of ATP were measured with the CellTiter Glo assay (Promega, Madison, WI), as previously described (Posimo et al., 2013; Posimo et al., 2014).

In order to determine the neuronal purity of the cultures, cells were immunocytochemically labeled for the neuronal marker MAP2 and the astrocyte marker glial fibrillary acidic protein (GFAP) using visible-range secondary antibodies for higher resolution microscopy, as previously described (Crum et al., 2015; Posimo et al., 2015). For the latter experiments, nuclei were stained with Hoechst 33258 (10 μg/mL, bisBenzimide) in phosphate-buffered saline with 0.3% Triton-X for 15 min. Photomicrographs were captured with an epifluorescent microscope (EVOS, Life Technologies) using the 20× objective (0.213 mm^2 field of view, three fields per well). An observer then counted the numbers of $MAP2^+$ cells and $Hoechst^+$ cells to determine neuron density in hippocampal cultures.

Statistical Analyses

Each experiment was run in at least three triplicate wells. The data from these three wells were averaged to yield an n of 1. Data are therefore presented as the mean and SEM from a minimum of 3 independent experiments. In order to reveal the spread of the values, all individual data points are also presented in Supplemental Information as scatterplots for key findings. The Grubb's outlier test was performed once on all the data. Depending upon the number of variables, data were analyzed by one, two, or three-way ANOVA followed by the Bonferroni *post hoc* correction (SPSS Version 20, Armonk, NY). Differences were deemed significant only when $p \leq 0.05$.

Results

We began this study by examining the phenotypic expression of neuronal and glial markers in primary hippocampal neuron cultures. As expected, our cultures contained cells immunopositive for the neuronal marker MAP2 as well as the astrocyte marker GFAP (Figure 1A). Counts of $MAP2^+$ and $Hoechst^+$ cells revealed that, on average, at least 76% of the hippocampal cultures were neuronal in phenotype (n = 4 independent experiments). Our previous work on olfactory bulb, neocortical, and entorhinal allocortical cultures is consistent with the observation that some astrocytes are present in postnatal cultures of brain cells (Crum et al., 2015; Posimo et al., 2013; Posimo et al., 2015). This observation probably reflects the peak of astrocyte births in the neonatal period (Bayer and Altman, 1991; Gotz, 2001; Okano and Temple, 2009).

Next we generated concentration-response curves for the proteasome inhibitor MG132 and the oxidative toxicant paraquat (Figure 1B–M). Both compounds were delivered on DIV5 or DIV6 and the treated cells were then assayed on DIV7. To be consistent with subsequent studies, the DIV5 treatment was referred to as the 1^{st} hit and the DIV6 treatment was referred to as the 2^{nd} hit. The 1^{st} hit of MG132 led to significant loss of the neuronal cytoskeletal marker MAP2 (Figure 1B, J) and ATP levels (Figure 1C) on DIV7 with little to no loss of the DRAQ5 stain for nuclei (not shown), suggesting that this model did not involve cell loss *per se* but involved loss of metabolic function and cytoskeletal integrity, both early markers of toxicity. MG132 was not highly toxic as a 2^{nd} hit when MAP2 levels were assayed 24h later on DIV7, but did elicit considerable loss of ATP (Figure 1D, K, E). The 1^{st} hit of paraquat led to significant loss of MAP2 (Figure F, L) and ATP (Figure 1G) at concentrations that led to little to no loss of DRAQ5-stained nuclei (not shown). Paraquat

was more toxic than MG132 when delivered as a 2nd hit at the concentrations tested, leading to significant loss of both MAP2 and ATP levels within 24h (Figure H, I, M).

Because of the relative lack of toxicity of the 2nd MG132 hit in Figure 1D, we combined a 1st hit of MG132 with a 2nd hit of paraquat instead of a 2nd hit of MG132 in order to determine whether the 1st hit would exacerbate the effect of the toxic 2nd hit. Thus, we pretreated hippocampal neurons with 0.125–1 μM MG132 24h prior to a 2nd hit with 100 μM paraquat (Figure 2A–D, I). However, MG132 and paraquat only exhibited additive toxic effects on DIV7. Although the MAP2 and ATP assays appeared to suggest that a 1st hit of high concentrations of MG132 (1 μM) prevented the response to a subsequent paraquat challenge, when the same data were graphed as a percentage of the 0 μM paraquat group (Figure 2C–D), it was evident that the 1st hit did not robustly change the effect of the 2nd hit at any concentration, according to any viability assay. These results suggest that the 1st hit of MG132 did not significantly shape the response to the 2nd hit of paraquat when hippocampal neurons were assayed for structural and metabolic fitness 24h after the final hit.

Next we combined a 1st hit of paraquat with a 2nd hit of the same toxicant and measured viability on DIV7 (Figure 2E–H, J). However, the effects of dual paraquat hits were also additive at this timepoint, except at the highest concentration of the 1st paraquat hit (50 μM) in the ATP assay (Figure 2F)—as is evident when expressing the same data as a percentage of the 0 μM 2nd hit group in Figure 2H. At this concentration, the ATP assay revealed that 1st hit blocked the loss of ATP in response to the 2nd hit, consistent with metabolic adaptations to oxidative stress. However, this compensatory pattern was not evident at the structural level with the MAP2 assay, which showed clearly that the 1st paraquat hit had no impact upon a 2nd paraquat hit when the data were expressed as a percentage of the 0 μM paraquat group (Figure 2E, G, J). It is worth noting here that the MAP2 assay is specific to neuronal elements whereas the ATP assay cannot distinguish between neuronal and glial profiles.

Our previous work showed that glutathione loss exacerbates the response to dual MG132 hits in primary cortical astrocytes (Gleixner et al., 2015; Titler et al., 2013) and that dual MG132 hits elicit synergistic loss of glutathione in neuroblastoma cells (Unnithan et al., 2012). As we observed no evidence of stress synergy thus far, we challenged the cells further by inhibiting glutathione synthesis with buthionine sulfoximine. However, no synergistic effects were evident with any viability assay on DIV7 (Figure S1). That is, the mild oxidative challenge of glutathione loss did not robustly change the impact of the 1st MG132 hit on the response to the 2nd paraquat hit (Figure S1A, B, F), as was evident when expressing the same data as a percentage of the 0 μM paraquat group (Figure S1D–E). Although the highest concentration of buthionine sulfoximine (25 μM) appeared to enhance the toxicity of 0.5 μM MG132 in the ATP assay in Figure S1E, the effect size was small and there was no convincing evidence for robust stress synergy between MG132 and paraquat. As expected, buthionine sulfoximine led to significant loss of glutathione levels (Figure S1C, G, H).

Thus far we had shown that dual hits were not synergistic within 24h of the last insult, even under conditions of glutathione loss. Our recent work showed that loss of heat shock protein activity leads to synergistic exacerbation of MG132 and/or lactacystin toxicity in cortical

and olfactory bulb neurons (Crum et al., 2015; Posimo et al., 2015). Hsp70 is thought to modulate the assembly of the proteasome under conditions of oxidative challenge (Grune et al., 2011). Thus, we inhibited the activity of the Hsp70/Hsc70 chaperone family to see if synergistic toxic effects of dual MG132/paraquat hits could be elicited. However, the Hsp70/Hsc70 activity inhibitor VER155008 did not elicit any synergy between dual hits of MG132 and paraquat (Figure S2). Instead, VER155008 exacerbated loss of MAP2 signal in MG132-pretreated cells (Figure S2A, E), supporting the view that Hsp70/Hsc70 and proteasome inhibitors are synergistic in their toxic effects when applied simultaneously. Similar results were observed with the ATP assay (Figure S2B). Surprisingly, in the presence of 25 μM VER155008, paraquat toxicity in MG132-pretreated cells was slightly ameliorated according to the MAP2 assay (Figure S2C), perhaps because 25 μM VER155008 was so toxic by itself that its administration enriched the cultures in highly resistant survivors that no longer responded to subsequent injury (see highly toxic effects of 25 μM VER155008 in Figure S2A). These findings confirm that loss of Hsp70 function synergizes with the toxicity of proteasome inhibitors but does not facilitate synergistic effects of dual oxidative and proteotoxic insults.

Thus far we had not observed synergistic toxic effects of sequential hits of MG132 followed by paraquat, or paraquat followed by a 2nd hit of the same toxicant. However, those data were all collected 24h after the 2nd hit, on DIV7. Therefore, we decided to repeat the experiments and assay viability on DIV8 to permit additional time for stress synergy to unfold. Furthermore, if we waited an additional 24h until DIV8, it might reveal toxicity of the 2nd hit of MG132, which was not yet evident on DIV7 (see Figure 1D). Consistent with these expectations, the 1st hit of MG132 exacerbated the loss of DRAQ5, MAP2, and ATP levels in response to the 2nd hit of paraquat when assessed on DIV8 (Figure 3). The loss of DRAQ5 nuclear staining suggested we were eliciting significant cell loss by this timepoint. In order to statistically evaluate the stress synergy, we also expressed the data as a percentage of the 0 μM 2nd paraquat hit group (Figure 3D–F). It is evident from those graphs that the 1st hit sensitized the cells to the 2nd hit according to all three assays when the survival period after the final hit was extended from 24 to 48h. Key findings here and in subsequent figures are graphed as scatterplots in Supplemental Figure S3 to show the full variability of these biological stress responses.

In our previous study on stress synergy in N2a cells, we had observed that the antioxidant NAC increased glutathione levels and prevented the synergistic toxic effects of dual MG132 hits (Unnithan et al., 2012). Thus, we examined whether NAC would prevent dual hit synergy in primary hippocampal neurons and measured glutathione levels. First we determined the optimally protective concentration of NAC by delivering a single hit of MG132 in the presence or absence of NAC and assaying viability on DIV7 (Figure 4A–B, D). NAC was found to be maximally protective against MAP2 loss at a concentration of 1 mM. At this concentration, NAC also facilitated an increase in ATP in response to MG132 (Figure 4B). Glutathione levels were not affected by NAC or MG132 when expressed as a function of the nuclear stain DRAQ5, supporting the view that NAC protected hippocampal neurons through a mechanism independent of glutathione synthesis in this model (Figure 4C, E), consistent with some previous studies (Jiang et al., 2013; Steenvoorden and Beijersburgen van Henegouwen, 1998).

Next we tested the hypothesis that NAC would protect against the synergistic toxicity of dual hits on DIV8 in the extended survival model shown in Figure 3. NAC did not protect against paraquat toxicity, but continued to mitigate the toxic effects of MG132 according to the MAP2 and ATP assays (Figure 4G–Q). Because of the lack of effect on paraquat toxicity, NAC also did not prevent the synergistic toxic effects of dual hits when MG132 was followed by paraquat. NAC did not significantly increase glutathione levels under these conditions (Figure 4J, N, Q), although there was a trend towards an increase in glutathione in NAC-treated cells after the 2nd hit of paraquat (Figure 4J, p=0.09, Bonferroni *post hoc*). In the normalized ATP data shown in Figure 4M, NAC appeared to slightly protect against ATP loss in the dual hit group. However, taken together, all the data demonstrate that NAC does not *robustly* protect against paraquat toxicity or against the synergistic toxicity of dual hits of MG132/paraquat.

Thus far we had shown that MG132 exacerbated paraquat toxicity when survival was extended to 48h after the final insult. Therefore, we tested the hypothesis that MG132 would also exacerbate the toxic response to a second hit of MG132 when assayed on DIV8. We had also shown that NAC protected against MG132. Thus, we applied the dual hits of MG132 in the absence or presence of NAC in our subsequent experiments (Figure 5). NAC prevented cell loss in response to MG132 according to the DRAQ5 assay (Figure 5A, E, I). The MAP2 assay for the neuronal cytoskeleton revealed slight synergy between the two hits of MG132 (Figure 5B, F, J). As expected, NAC prevented MAP2 loss in response to both single and dual hits of MG132 (Figure 5B, F, J). Dual hits of MG132 did not lead to synergistic loss of ATP (Figure 5C, G). NAC prevented the loss of ATP in response to the 2nd hit of MG132, consistent with the MAP2 and DRAQ5 data. However, when the data were expressed as a percentage of the 0 μM 2nd hit group in Figures 5E and 5G, it became evident that NAC failed to prevent DRAQ5 and ATP loss in the dual hit group. There were no significant changes in glutathione levels in Figure 5D, but when the glutathione values were expressed as a percentage of the 0 μM 2nd hit group in Figure 5H, it was apparent that dual hits elicited mild glutathione loss and that NAC prevented this synergistic effect. However, the size of this effect was moderate and the effect was too variable to be statistically evident in Figure 5D.

Because dual hits of MG132 were not robustly synergistic in Figure 5, we decided to vary the concentration of the 2nd hit and repeat the extended survival experiment (Figure 6). Stress synergy was indeed evident when the MAP2 and ATP data were expressed as a function of the 0 μM 2nd hit group (Figure 6E, F). That is, cells treated with 0.5 μM MG132 as a 1st hit were much more vulnerable to 1 μM MG132 delivered as a 2nd hit than control cells. The effect sizes were larger than in Figure 5, perhaps due to variability in the quality of the neuron cultures or the potency of the frozen stock solutions. In contrast to the MAP2 and ATP data, stress synergy was not evident with the DRAQ5 assay following dual MG132 hits, consistent with data shown in Figure 5. In sum, stress synergy following exposure to dual hits of MG132 is not the default response but depends on the measurement or viability assay employed.

Discussion

The two hit hypothesis of neurodegeneration has been proposed as a model for both Alzheimer's and Parkinson's disease (Boger et al., 2010; Cory-Slechta et al., 2005; Gao et al., 2011; Hawkes et al., 2007; Zhu et al., 2007). As neurodegenerative disorders are known to progress over the course of decades, it seems highly likely that cells in vulnerable brain regions would be exposed to more than one insult. Indeed, Gu and colleagues have argued that individuals who are not exposed to more than one hit do not actually progress towards full-blown Parkinson's disease (Gu et al., 1998). Boger and colleagues have shown that loss of neurotrophic factors can synergize with age-related declines in dopaminergic systems or with neurotoxicant exposures and thereby elicit parkinsonism (Boger et al., 2010). It has also been reported that Alzheimer's-related pathology predisposes cells towards increased vulnerability to kindling or seizure-associated cell death (Chan et al., 2015; Faa et al., 2014) and that alpha-synucleinopathy and pro-inflammatory factors can work in synergy to potentiate Parkinson's pathology (Gao et al., 2011). Several studies further support the view that exposure to stress early in life predisposes the brain to neurodegeneration later in life, perhaps through inflammatory and epigenetic changes (Carvey et al., 2006; Faa et al., 2014; Ling et al., 2004; Ling et al., 2006). For example, traumatic brain injury is thought to predispose the brain to future insults and increase risk for neurodegenerative disorders (Gupta and Sen, 2015). Nuclear trafficking deficits in proteins such as TDP-43 and FUS are proposed to act in combination with multiple other hits, such as cellular stressors or genetic vulnerabilities, perhaps culminating in amyotrophic lateral sclerosis or frontotemporal lobar degeneration (Dormann and Haass, 2011). If the two hit hypothesis gains support in epidemiological human studies, it would be vital to protect at-risk individuals against subsequent hits in order to prevent the initiation of neurodegenerative processes.

To our knowledge, the present study is the first to show that neurons of the hippocampus, when exposed to severe proteotoxic stress, die more readily in response to a second hit of oxidative stress, but only in a delayed fashion. The synergistic effects of dual hits in our model were not immediate and unfolded between 24h and 48h after the final hit, revealing the importance of the choice of timepoint for conducting viability assays *in vitro*. It is entirely possible that we would have observed even greater synergy had we extended the survival to DIV9. Dual MG132 hits consistently failed to elicit synergistic loss of cells in the DRAQ5 assay. Furthermore, dual hits of MG132 only synergized at some and not all concentrations. Although some of our findings are consistent with the dual hit hypothesis, stress synergy was by no means the default response. Rather, conditions had to be optimized for endogenous defenses to fail in this cell type and multiple viability assays had to be employed to capture synergistic stress responses. As expected, the most reproducible findings were gleaned from the MAP2 assay, perhaps because it is specific to neuronal elements, unlike the other two measurements, which are sensitive to variable levels of glial hyperplasia. Taken together, these findings strongly suggest that the duration of survival after the injury, the type and degree of the original insult, and the nature of the viability measurement all profoundly influence the elaboration of synergistic stress responses in cells from the hippocampus.

As mentioned above, the synergy of sequential hits of proteotoxic and oxidative stress was evident within 48h of the second hit. There are several potential mechanistic explanations for the synergy between two distinct types of stress. First, oxidative stress has been shown to decrease proteasomal activity (Keller et al., 2000b). Conversely, proteasome inhibition induces reactive oxygen species production (Papa and Rockwell, 2008) and has been shown to sensitize dopamine neurons to oxidative injury, perhaps by potentiating mitochondrial energy depletion after inhibition of complex I (Hoglinger et al., 2003; Mytilineou et al., 2004). In addition, the proteasome is intimately involved in protection against oxidative imbalance, perhaps because cells degrade oxidized proteins through the proteasome particle in an Nrf2-dependent manner (Pickering et al., 2012). Another explanation for the observed stress synergy might be loss of mitochondrial function and inhibition of glucose utilization. In this context, stress-responsive glucocorticoids have been shown to exacerbate cell death via inhibition of glucose utilization in hippocampal neurons treated with a variety of oxidative and excitotoxic insults (Sapolsky et al., 1988). Further studies of the mechanisms underlying stress sensitization are warranted, as we did not collect robust evidence that glutathione down- or upregulation determined the direction of the stress response in the present model.

Considering our previous findings on stress resistance in astrocytes versus the stress synergy we reported in neuroblastoma cells (Gleixner et al., 2015; Titler et al., 2013; Unnithan et al., 2012; Unnithan et al., 2014), the present findings lend further support to the notion that cell type influences the direction of the stress response. Even more specifically, brain subregion and neuronal subtype may also determine whether the stress response takes a toxic turn. This view is supported by previous studies on telencephalic neurons showing that cortical subregion (*e.g.* entorhinal allocortex versus sensorimotor neocortex) and cell type (astrocyte versus neuron) impact the toxic response to proteotoxic and oxidative stressors (Posimo et al., 2013; Posimo et al., 2015).

NAC has been available in inexpensive capsule form for several decades and is one of the most widely used positive control in studies of neuroprotection, suggesting a broad range of therapeutic effects. In the present study, NAC was found to prevent the toxicity of single MG132 hits. Although NAC failed to prevent DRAQ5 and ATP loss after dual MG132 hits, it dramatically ameliorated MAP2 loss, the only marker specific for neurons (see Figure 5B, J). These findings are consistent with previous reports that NAC significantly prevents the toxicity of proteasome inhibitors (Jiang et al., 2013; Papa and Rockwell, 2008; Posimo et al., 2013; Unnithan et al., 2012). Because disruptions in glutathione metabolism are common in brain disorders, NAC has been used to treat several neurological and psychiatric conditions with some success (Berk et al., 2008a; Hoffer et al., 2013); (Adair et al., 2001; Berk et al., 2008b). Although NAC efficacy is often thought to be based on glutathione, our recent data suggest that it can exert both glutathione-dependent (Posimo et al., 2013; Unnithan et al., 2012; Unnithan et al., 2014) and glutathione-independent modes of action (Jiang et al., 2013). In the present study, NAC did not prevent paraquat toxicity. In this context, it is important to note that NAC did not increase glutathione levels in paraquat-treated cells and that multiple authors have argued that NAC can exert pro-oxidant effects under some circumstances (Finn and Kemp, 2012; Harvey et al., 2008; Sagrista et al., 2002). NAC did slightly increase glutathione in the cells treated with dual hits of MG132, consistent with our

previous findings in neuroblastoma cells showing that NAC prevented a synergistic loss of glutathione defenses in cells hit twice with MG132 (Unnithan et al., 2012). These data may explain why NAC was effective against MG132 but not paraquat.

Several limitations of the present study must be conceded. First, the number of insults that lead individuals down the path of inexorable neurodegeneration is obviously not necessarily exactly two. Thus, the use of two hits in the present study was for proof of principle only. It is more likely that there are multiple recurring insults over the course of a lifetime that lay the foundation for the progressive accumulation of damage in the aged human brain. For example, as stated above, the diseased brain may be exposed to inflammation as well as loss of metal, redox, and protein homeostasis. Although some authors have argued in favor of a one hit hypothesis instead of a dual hit hypothesis (Clarke et al., 2000), many more others have argued in favor of multiple hits (Boger et al., 2010; Cory-Slechta et al., 2005; Dormann and Haass, 2011; Gao et al., 2011; Hawkes et al., 2007; Zhu et al., 2007). Although two hits are minimally sufficient to determine whether synergistic, additive, or refractory stress responses are elicited, future use of triple and quadruple sequential hits might serve to develop even more rigorous models to examine the therapeutic potential of novel drugs.

The second limitation of the present study is that the experiments were not conducted in intact animals and the toxicant exposures were therefore not systemic. Connections with other brain regions are lost in dissociated primary cultures of neurons and the isolated cells are exposed to highly artificial conditions. One might even argue that primary hippocampal neurons are more prone to die than they would be *in vivo* because of the artificial conditions they are subjected to *in vitro* and that stress exacerbation is more readily achieved in a primary culture model than in the intact brain.

The third limitation of the present study is that we applied our stressors sequentially to test for sensitization to subsequent insults, whereas neurodegenerative disorders may involve simultaneous exposures to multiple different types of stress, ranging from concurrent proteotoxic and oxidative stress to inflammation and loss of metal homeostasis, all of which may propagate each other in a self-perpetuating loop. This heterogeneity of concomitant insults may partly explain why neurological disorders such as Alzheimer’s and Parkinson’s disease are only poorly controlled with available therapies. Therefore, it might be worthwhile to apply combinations of MG132, paraquat, lipopolysaccharide, iron, and rotenone simultaneously to neurons at low concentrations over longer time periods as an alternative protocol for stress synergy. This would be the natural extension of a recent study in SH-SY5Y cells reporting synergistic toxic responses to paired oxidative, mitochondrial, proteasomal, and lysosomal insults (Yong-Kee et al., 2012).

The fourth limitation of the present report is that we have not modeled endogenous toxic factors, such as genetic and epigenetic vulnerabilities, that contribute to neurodegeneration in humans. To address this limitation, transgenic mouse models would be useful to reveal if there is an impact of familial Parkinson’s and Alzheimer’s mutations on the response to multiple hits of proteotoxic and oxidative stressors in aging animals. Some studies have already shown that these mutations exacerbate the response to single hits (for some examples, see Nieto et al., 2006; Song et al., 2004).

One of the strengths of the present study is the use of three independent assays for quantifying cellular viability. These assays have been shown to be linearly correlated with cell density in previous studies (Posimo et al., 2013; Posimo et al., 2014; Unnithan et al., 2012). It is important to conduct multiple assays for viability because cellular integrity is multifaceted and the assays are not always in agreement. For example, changes in metabolic viability or ATP levels do not always parallel changes in cell numbers (Posimo et al., 2013; Posimo et al., 2014; Titler et al., 2013; Unnithan et al., 2012). Therefore, we do not view the results of the ATP assay as a measure of cell density but only as a measure of metabolic fitness. Furthermore, the DRAQ5 assay is less sensitive than the MAP2 assay, perhaps because glial cells are also stained by this marker and are less vulnerable than $MAP2^{+}$ neuronal profiles. The DRAQ5 results were nevertheless useful in that we were able to show synergistic cell loss after dual hits, providing concrete evidence of stress exacerbation in hippocampal cultures. A thorough discussion of the weaknesses and strengths of these assays can be found in our previous reports (Posimo et al., 2014; Unnithan et al., 2012).

In conclusion, we have performed an extensive study to characterize the nature of the stress response to dual hits of oxidative and proteotoxic stressors in cells from the vulnerable hippocampus. In order to strengthen our interpretations, we have applied four types of stress (inhibitors of proteasomes, Hsp70/Hsc70, and glutathione as well as an oxidative toxicant), used three independent and unbiased viability assays, and made measurements at multiple timepoints. The present findings support the view that hippocampal neurons are even more vulnerable to injury if loss of protein homeostasis is followed by loss of redox homeostasis and that NAC supplementation can protect hippocampal neurons against some but not all types of injuries. This phenomenon of stress exacerbation in neurons lies in contrast to the stress tolerance exhibited by primary astrocytes when exposed to dual proteotoxic hits, supporting the view that neurons are more vulnerable to stress exacerbation (Gleixner et al., 2015; Titler et al., 2013). The new model presented here also serves as a robust method to test potential therapies, because treatments that can protect against unremitting, severe stress are more likely to succeed in the clinic, where exposures to stress in real life almost never occur in isolation or as singular events.

Supplementary Material

Refer to Web version on PubMed Central for supplementary material.

Acknowledgments

Designed the experiments and wrote the paper: RKL. Conducted the experiments: SDH, JMP, DMM, and DFH. Analyzed the data and generated figures and tables: SDH. We are grateful to Mary Caruso, Deborah Willson, and Jackie Farrer for excellent administrative support. We are also grateful for Denise Butler-Buccilli and Christine Close for outstanding animal care. This study was supported by NINDS grant R15NS093539 (RKL), NINDS grant R03NS088395 (RKL), and Hillman foundation GRANT109033 (RKL).

Abbreviations

DMSO	dimethyl sulfoxide
MAP2	microtubule associated protein 2

PBS	phosphate-buffered saline
TBS	Tris-buffered saline

References

Adair JC, Knoefel JE, Morgan N. Controlled trial of N-acetylcysteine for patients with probable Alzheimer's disease. Neurology. 2001; 57(8):1515–7. [PubMed: 11673605]

Anne Stetler R, Leak RK, Gao Y, Chen J. The dynamics of the mitochondrial organelle as a potential therapeutic target. J Cereb Blood Flow Metab. 2013; 33(1):22–32. [PubMed: 23093069]

Bayer, SA.; Altman, J. Neocortical Development. New York: Raven Press; 1991. p. xivp. 255

Berk M, Copolov D, Dean O, Lu K, Jeavons S, Schapkaitz I, Anderson-Hunt M, Judd F, Katz F, Katz P, et al. N-acetyl cysteine as a glutathione precursor for schizophrenia--a double-blind, randomized, placebo-controlled trial. Biological psychiatry. 2008a; 64(5):361–8. [PubMed: 18436195]

Berk M, Copolov DL, Dean O, Lu K, Jeavons S, Schapkaitz I, Anderson-Hunt M, Bush AI. N-acetyl cysteine for depressive symptoms in bipolar disorder--a double-blind randomized placebo-controlled trial. Biological psychiatry. 2008b; 64(6):468–75. [PubMed: 18534556]

Bertrand E, Lechowicz W, Szpak GM, Lewandowska E, Dymecki J, Wierzba-Bobrowicz T. Limbic neuropathology in idiopathic Parkinson's disease with concomitant dementia. Folia Neuropathol. 2004; 42(3):141–50. [PubMed: 15535032]

Beyer MK, Bronnick KS, Hwang KS, Bergsland N, Tysnes OB, Larsen JP, Thompson PM, Somme JH, Apostolova LG. Verbal memory is associated with structural hippocampal changes in newly diagnosed Parkinson's disease. J Neurol Neurosurg Psychiatry. 2013; 84(1):23–8. [PubMed: 23154124]

Blesa J, Phani S, Jackson-Lewis V, Przedborski S. Classic and new animal models of Parkinson's disease. J Biomed Biotechnol. 2012; 2012:845618. [PubMed: 22536024]

Blesa J, Trigo-Damas I, Quiroga-Varela A, Jackson-Lewis VR. Oxidative stress and Parkinson's disease. Front Neuroanat. 2015; 9:91. [PubMed: 26217195]

Boger HA, Granholm AC, McGinty JF, Middaugh LD. A dual-hit animal model for age-related parkinsonism. Progress in neurobiology. 2010; 90(2):217–29. [PubMed: 19853012]

Braak H, Braak E. Staging of Alzheimer's disease-related neurofibrillary changes. Neurobiol Aging. 1995; 16(3):271–8. discussion 278–84. [PubMed: 7566337]

Braak H, Braak E. Diagnostic criteria for neuropathologic assessment of Alzheimer's disease. Neurobiol Aging. 1997a; 18(4 Suppl):S85–8. [PubMed: 9330992]

Braak H, Braak E. Frequency of stages of Alzheimer-related lesions in different age categories. Neurobiol Aging. 1997b; 18(4):351–7. [PubMed: 9330961]

Braak H, Braak E, Bohl J. Staging of Alzheimer-related cortical destruction. Eur Neurol. 1993; 33(6): 403–8. [PubMed: 8307060]

Braak H, Del Tredici K, Bohl J, Bratzke H, Braak E. Pathological changes in the parahippocampal region in select non-Alzheimer's dementias. Ann N Y Acad Sci. 2000a; 911:221–39. [PubMed: 10911877]

Braak H, Del Tredici K, Bratzke H, Hamm-Clement J, Sandmann-Keil D, Rub U. Staging of the intracerebral inclusion body pathology associated with idiopathic Parkinson's disease (preclinical and clinical stages). J Neurol. 2002; 249(Suppl 3):III/1–5.

Braak H, Del Tredici K, Rub U, de Vos RA, Jansen Steur EN, Braak E. Staging of brain pathology related to sporadic Parkinson's disease. Neurobiol Aging. 2003; 24(2):197–211. [PubMed: 12498954]

Braak H, Del Tredici K, Schultz C, Braak E. Vulnerability of select neuronal types to Alzheimer's disease. Ann N Y Acad Sci. 2000b; 924:53–61. [PubMed: 11193802]

Camicioli R, Moore MM, Kinney A, Corbridge E, Glassberg K, Kaye JA. Parkinson's disease is associated with hippocampal atrophy. Mov Disord. 2003; 18(7):784–90. [PubMed: 12815657]

Carvey PM, Punati A, Newman MB. Progressive dopamine neuron loss in Parkinson's disease: the multiple hit hypothesis. Cell Transplant. 2006; 15(3):239–50. [PubMed: 16719059]

Chan J, Jones NC, Bush AI, O'Brien TJ, Kwan P. A mouse model of Alzheimer's disease displays increased susceptibility to kindling and seizure-associated death. Epilepsia. 2015

Chen Q, Niu Y, Zhang R, Guo H, Gao Y, Li Y, Liu R. The toxic influence of paraquat on hippocampus of mice: involvement of oxidative stress. Neurotoxicology. 2010; 31(3):310–6. [PubMed: 20211647]

Clarke G, Collins RA, Leavitt BR, Andrews DF, Hayden MR, Lumsden CJ, McInnes RR. A one-hit model of cell death in inherited neuronal degenerations. Nature. 2000; 406(6792):195–9. [PubMed: 10910361]

Cocheme HM, Murphy MP. Complex I is the major site of mitochondrial superoxide production by paraquat. J Biol Chem. 2008; 283(4):1786–98. [PubMed: 18039652]

Cory-Slechta DA, Thiruchelvam M, Barlow BK, Richfield EK. Developmental pesticide models of the Parkinson disease phenotype. Environ Health Perspect. 2005; 113(9):1263–70. [PubMed: 16140639]

Crum TS, Gleixner AM, Posimo JM, Mason DM, Broeren MT, Heinemann SD, Wipf P, Brodsky JL, Leak RK. Heat shock protein responses to aging and proteotoxicity in the olfactory bulb. J Neurochem. 2015

Dalton VS, Verdurand M, Walker A, Hodgson DM, Zavitsanou K. Synergistic Effect between Maternal Infection and Adolescent Cannabinoid Exposure on Serotonin 5HT1A Receptor Binding in the Hippocampus: Testing the "Two Hit" Hypothesis for the Development of Schizophrenia. ISRN Psychiatry. 2012; 2012:451865. [PubMed: 23738203]

Depaulis A, Hamelin S. Animal models for mesiotemporal lobe epilepsy: The end of a misunderstanding? Rev Neurol (Paris). 2015; 171(3):217–26. [PubMed: 25748330]

Dormann D, Haass C. TDP-43 and FUS: a nuclear affair. Trends Neurosci. 2011; 34(7):339–48. [PubMed: 21700347]

Faa G, Marcialis MA, Ravarino A, Piras M, Pintus MC, Fanos V. Fetal programming of the human brain: is there a link with insurgence of neurodegenerative disorders in adulthood? Curr Med Chem. 2014; 21(33):3854–76. [PubMed: 24934353]

Finn NA, Kemp ML. Pro-oxidant and antioxidant effects of N-acetylcysteine regulate doxorubicin-induced NF-kappa B activity in leukemic cells. Mol Biosyst. 2012; 8(2):650–62. [PubMed: 22134636]

Gao HM, Zhang F, Zhou H, Kam W, Wilson B, Hong JS. Neuroinflammation and alpha-synuclein dysfunction potentiate each other, driving chronic progression of neurodegeneration in a mouse model of Parkinson's disease. Environmental health perspectives. 2011; 119(6):807–14. [PubMed: 21245015]

Gleixner AM, Posimo JM, Pant DB, Henderson MP, Leak RK. Astrocytes Surviving Severe Stress Can Still Protect Neighboring Neurons from Proteotoxic Injury. Mol Neurobiol. 2015

Gomez-Isla T, Hollister R, West H, Mui S, Growdon JH, Petersen RC, Parisi JE, Hyman BT. Neuronal loss correlates with but exceeds neurofibrillary tangles in Alzheimer's disease. Ann Neurol. 1997; 41(1):17–24. [PubMed: 9005861]

Gotz M. Cerebral Cortex Development. Encyclopedia of Life Sciences. 2001:1–7.

Griffith OW. Mechanism of action, metabolism, and toxicity of buthionine sulfoximine and its higher homologs, potent inhibitors of glutathione synthesis. The Journal of biological chemistry. 1982; 257(22):13704–12. [PubMed: 6128339]

Grune T, Catalgol B, Licht A, Ermak G, Pickering AM, Ngo JK, Davies KJ. HSP70 mediates dissociation and reassociation of the 26S proteasome during adaptation to oxidative stress. Free Radic Biol Med. 2011; 51(7):1355–64. [PubMed: 21767633]

Gu M, Owen AD, Toffa SE, Cooper JM, Dexter DT, Jenner P, Marsden CD, Schapira AH. Mitochondrial function, GSH and iron in neurodegeneration and Lewy body diseases. J Neurol Sci. 1998; 158(1):24–9. [PubMed: 9667773]

Gupta R, Sen N. Traumatic brain injury: a risk factor for neurodegenerative diseases. Rev Neurosci. 2015

Hamelin S, Depaulis A. Revisiting hippocampal sclerosis in mesial temporal lobe epilepsy according to the "two-hit" hypothesis. Rev Neurol (Paris). 2015; 171(3):227–35. [PubMed: 25748332]

Harvey BH, Joubert C, du Preez JL, Berk M. Effect of chronic N-acetyl cysteine administration on oxidative status in the presence and absence of induced oxidative stress in rat striatum. Neurochem Res. 2008; 33(3):508–17. [PubMed: 17763945]

Hawkes CH, Del Tredici K, Braak H. Parkinson's disease: a dual-hit hypothesis. Neuropathol Appl Neurobiol. 2007; 33(6):599–614. [PubMed: 17961138]

Hill RA, Klug M, Kiss Von Soly S, Binder MD, Hannan AJ, van den Buuse M. Sex-specific disruptions in spatial memory and anhedonia in a "two hit" rat model correspond with alterations in hippocampal brain-derived neurotrophic factor expression and signaling. Hippocampus. 2014; 24(10):1197–211. [PubMed: 24802968]

Hoffer ME, Balaban C, Slade MD, Tsao JW, Hoffer B. Amelioration of acute sequelae of blast induced mild traumatic brain injury by N-acetyl cysteine: a double-blind, placebo controlled study. PLoS One. 2013; 8(1):e54163. [PubMed: 23372680]

Hoffmann AF, Zhao Q, Holmes GL. Cognitive impairment following status epilepticus and recurrent seizures during early development: support for the "two-hit hypothesis". Epilepsy Behav. 2004; 5(6):873–7. [PubMed: 15582835]

Hoglinger GU, Carrard G, Michel PP, Medja F, Lombes A, Ruberg M, Friguet B, Hirsch EC. Dysfunction of mitochondrial complex I and the proteasome: interactions between two biochemical deficits in a cellular model of Parkinson's disease. J Neurochem. 2003; 86(5):1297–307. [PubMed: 12911637]

Jiang Y, Rumble JL, Gleixner AM, Unnithan AS, Pulugulla SH, Posimo JM, Choi HJ, Crum TS, Pant DB, Leak RK. N-Acetyl cysteine blunts proteotoxicity in a heat shock protein-dependent manner. Neuroscience. 2013; 255C:19–32. [PubMed: 24096134]

Jones BC, Huang X, Mailman RB, Lu L, Williams RW. The perplexing paradox of paraquat: the case for host-based susceptibility and postulated neurodegenerative effects. J Biochem Mol Toxicol. 2014; 28(5):191–7. [PubMed: 24599642]

Jucker M, Walker LC. Self-propagation of pathogenic protein aggregates in neurodegenerative diseases. Nature. 2013; 501(7465):45–51. [PubMed: 24005412]

Kalaitzakis ME, Christian LM, Moran LB, Graeber MB, Pearce RK, Gentleman SM. Dementia and visual hallucinations associated with limbic pathology in Parkinson's disease. Parkinsonism Relat Disord. 2009; 15(3):196–204. [PubMed: 18602855]

Kandiah N, Zainal NH, Narasimhalu K, Chander RJ, Ng A, Mak E, Au WL, Sitoh YY, Nadkarni N, Tan LC. Hippocampal volume and white matter disease in the prediction of dementia in Parkinson's disease. Parkinsonism Relat Disord. 2014; 20(11):1203–8. [PubMed: 25258331]

Keller JN, Hanni KB, Markesbery WR. Impaired proteasome function in Alzheimer's disease. J Neurochem. 2000a; 75(1):436–9. [PubMed: 10854289]

Keller JN, Hanni KB, Markesbery WR. Possible involvement of proteasome inhibition in aging: implications for oxidative stress. Mech Ageing Dev. 2000b; 113(1):61–70. [PubMed: 10708250]

Kim GH, Kim JE, Rhie SJ, Yoon S. The Role of Oxidative Stress in Neurodegenerative Diseases. Exp Neurobiol. 2015; 24(4):325–40. [PubMed: 26713080]

Leak RK. Adaptation and sensitization to proteotoxic stress. Dose-response : a publication of International Hormesis Society. 2014; 12(1):24–56. [PubMed: 24659932]

Leak RK, Liou AK, Zigmond MJ. Effect of sublethal 6-hydroxydopamine on the response to subsequent oxidative stress in dopaminergic cells: evidence for preconditioning. J Neurochem. 2006; 99(4):1151–63. [PubMed: 16956375]

Leak RK, Zigmond MJ, Liou AK. Adaptation to chronic MG132 reduces oxidative toxicity by a CuZnSOD-dependent mechanism. J Neurochem. 2008; 106(2):860–74. [PubMed: 18466318]

Lee DH, Goldberg AL. Proteasome inhibitors: valuable new tools for cell biologists. Trends Cell Biol. 1998; 8(10):397–403. [PubMed: 9789328]

Lewis DV. Losing neurons: selective vulnerability and mesial temporal sclerosis. Epilepsia. 2005; 46(Suppl 7):39–44. [PubMed: 16201994]

Ling Z, Chang QA, Tong CW, Leurgans SE, Lipton JW, Carvey PM. Rotenone potentiates dopamine neuron loss in animals exposed to lipopolysaccharide prenatally. Experimental neurology. 2004; 190(2):373–83. [PubMed: 15530876]

Ling Z, Zhu Y, Tong C, Snyder JA, Lipton JW, Carvey PM. Progressive dopamine neuron loss following supra-nigral lipopolysaccharide (LPS) infusion into rats exposed to LPS prenatally. Exp Neurol. 2006; 199(2):499–512. [PubMed: 16504177]

Llorente R, Miguel-Blanco C, Aisa B, Lachize S, Borcel E, Meijer OC, Ramirez MJ, De Kloet ER, Viveros MP. Long term sex-dependent psychoneuroendocrine effects of maternal deprivation and juvenile unpredictable stress in rats. J Neuroendocrinol. 2011; 23(4):329–44. [PubMed: 21219484]

Massey AJ, Williamson DS, Browne H, Murray JB, Dokurno P, Shaw T, Macias AT, Daniels Z, Geoffroy S, Dopson M, et al. A novel, small molecule inhibitor of Hsc70/Hsp70 potentiates Hsp90 inhibitor induced apoptosis in HCT116 colon carcinoma cells. Cancer chemotherapy and pharmacology. 2010; 66(3):535–45. [PubMed: 20012863]

McCarley RW, Wible CG, Frumin M, Hirayasu Y, Levitt JJ, Fischer IA, Shenton ME. MRI anatomy of schizophrenia. Biol Psychiatry. 1999; 45(9):1099–119. [PubMed: 10331102]

McEwen BS. Plasticity of the hippocampus: adaptation to chronic stress and allostatic load. Ann N Y Acad Sci. 2001; 933:265–77. [PubMed: 12000027]

McEwen BS, Magarinos AM. Stress effects on morphology and function of the hippocampus. Ann N Y Acad Sci. 1997; 821:271–84. [PubMed: 9238211]

McNaught KS, Belizaire R, Jenner P, Olanow CW, Isacson O. Selective loss of 20S proteasome alpha-subunits in the substantia nigra pars compacta in Parkinson's disease. Neurosci Lett. 2002; 326(3): 155–8. [PubMed: 12095645]

McNaught KS, Jenner P. Proteasomal function is impaired in substantia nigra in Parkinson's disease. Neurosci Lett. 2001; 297(3):191–4. [PubMed: 11137760]

Mytilineou C, McNaught KS, Shashidharan P, Yabut J, Baptiste RJ, Parnandi A, Olanow CW. Inhibition of proteasome activity sensitizes dopamine neurons to protein alterations and oxidative stress. J Neural Transm. 2004; 111(10–11):1237–51. [PubMed: 15480836]

Navarro A, Boveris A. Brain mitochondrial dysfunction in aging, neurodegeneration, and Parkinson's disease. Front Aging Neurosci. 2010; 2

Navarro A, Lopez-Cepero JM, Bandez MJ, Sanchez-Pino MJ, Gomez C, Cadenas E, Boveris A. Hippocampal mitochondrial dysfunction in rat aging. Am J Physiol Regul Integr Comp Physiol. 2008; 294(2):R501–9. [PubMed: 18077512]

Nieto M, Gil-Bea FJ, Dalfo E, Cuadrado M, Cabodevilla F, Sanchez B, Catena S, Sesma T, Ribe E, Ferrer I, et al. Increased sensitivity to MPTP in human alpha-synuclein A30P transgenic mice. Neurobiol Aging. 2006; 27(6):848–56. [PubMed: 16006012]

Nikonenko AG, Radenovic L, Andjus PR, Skibo GG. Structural features of ischemic damage in the hippocampus. Anat Rec (Hoboken). 2009; 292(12):1914–21. [PubMed: 19943345]

Okano H, Temple S. Cell types to order: temporal specification of CNS stem cells. Curr Opin Neurobiol. 2009; 19(2):112–9. [PubMed: 19427192]

Ouardouz M, Lema P, Awad PN, Di Cristo G, Carmant L. N-methyl-D-aspartate, hyperpolarization-activated cation current (Ih) and gamma-aminobutyric acid conductances govern the risk of epileptogenesis following febrile seizures in rat hippocampus. Eur J Neurosci. 2010; 31(7):1252–60. [PubMed: 20345922]

Papa L, Rockwell P. Persistent mitochondrial dysfunction and oxidative stress hinder neuronal cell recovery from reversible proteasome inhibition. Apoptosis. 2008; 13(4):588–99. [PubMed: 18299995]

Pickering AM, Linder RA, Zhang H, Forman HJ, Davies KJ. Nrf2-dependent induction of proteasome and Pa28alphabeta regulator are required for adaptation to oxidative stress. J Biol Chem. 2012; 287(13):10021–31. [PubMed: 22308036]

Posimo JM, Titler AM, Choi HJ, Unnithan AS, Leak RK. Neocortex and allocortex respond differentially to cellular stress in vitro and aging in vivo. PLoS One. 2013; 8(3):e58596. [PubMed: 23536801]

Posimo JM, Unnithan AS, Gleixner AM, Choi HJ, Jiang Y, Pulugulla SH, Leak RK. Viability assays for cells in culture. Journal of visualized experiments : JoVE. 2014; 83(83):e50645. [PubMed: 24472892]

Posimo JM, Weilnau JN, Gleixner AM, Broeren MT, Weiland NL, Brodsky JL, Wipf P, Leak RK. Heat shock protein defenses in the neocortex and allocortex of the telencephalon. Neurobiol Aging. 2015; 36(5):1924–37. [PubMed: 25771395]

Raskin J, Cummings J, Hardy J, Schuh K, Dean RA. Neurobiology of Alzheimer's Disease: Integrated Molecular, Physiological, Anatomical, Biomarker, and Cognitive Dimensions. Curr Alzheimer Res. 2015; 12(8):712–22. [PubMed: 26412218]

Rideout HJ, Larsen KE, Sulzer D, Stefanis L. Proteasomal inhibition leads to formation of ubiquitin/alpha-synuclein-immunoreactive inclusions in PC12 cells. J Neurochem. 2001; 78(4):899–908. [PubMed: 11520910]

Rideout HJ, Stefanis L. Proteasomal inhibition-induced inclusion formation and death in cortical neurons require transcription and ubiquitination. Mol Cell Neurosci. 2002; 21(2):223–38. [PubMed: 12401444]

Sagrista ML, Garcia AE, Africa De Madariaga M, Mora M. Antioxidant and pro-oxidant effect of the thiolic compounds N-acetyl-L-cysteine and glutathione against free radical-induced lipid peroxidation. Free Radic Res. 2002; 36(3):329–40. [PubMed: 12071352]

Sapolsky RM, Packan DR, Vale WW. Glucocorticoid toxicity in the hippocampus: in vitro demonstration. Brain Res. 1988; 453(1–2):367–71. [PubMed: 3401775]

Schlecht R, Scholz SR, Dahmen H, Wegener A, Sirrenberg C, Musil D, Bomke J, Eggenweiler HM, Mayer MP, Bukau B. Functional analysis of Hsp70 inhibitors. PLoS One. 2013; 8(11):e78443. [PubMed: 24265689]

Schroder J, Pantel J. Neuroimaging of hippocampal atrophy in early recognition of Alzheimer s disease - a critical appraisal after two decades of research. Psychiatry Res. 2016; 247:71–8. [PubMed: 26774855]

Selye, H. Stress without distress. Philadelphia: Signet; 1975.

Somera-Molina KC, Robin B, Somera CA, Anderson C, Stine C, Koh S, Behanna HA, Van Eldik LJ, Watterson DM, Wainwright MS. Glial activation links early-life seizures and long-term neurologic dysfunction: evidence using a small molecule inhibitor of proinflammatory cytokine upregulation. Epilepsia. 2007; 48(9):1785–800. [PubMed: 17521344]

Song DD, Shults CW, Sisk A, Rockenstein E, Masliah E. Enhanced substantia nigra mitochondrial pathology in human alpha-synuclein transgenic mice after treatment with MPTP. Exp Neurol. 2004; 186(2):158–72. [PubMed: 15026254]

Steenvoorden DP, Beijersburgen van Henegouwen GM. Glutathione synthesis is not involved in protection by N-acetylcysteine against UVB-induced systemic immunosuppression in mice. Photochem Photobiol. 1998; 68(1):97–100. [PubMed: 9679454]

Sun F, Anantharam V, Zhang D, Latchoumycandane C, Kanthasamy A, Kanthasamy AG. Proteasome inhibitor MG-132 induces dopaminergic degeneration in cell culture and animal models. Neurotoxicology. 2006; 27(5):807–15. [PubMed: 16870259]

Tanner CM, Kamel F, Ross GW, Hoppin JA, Goldman SM, Korell M, Marras C, Bhudhikanok GS, Kasten M, Chade AR, et al. Rotenone, paraquat, and Parkinson's disease. Environ Health Perspect. 2011; 119(6):866–72. [PubMed: 21269927]

Titler AM, Posimo JM, Leak RK. Astrocyte plasticity revealed by adaptations to severe proteotoxic stress. Cell and tissue research. 2013; 352(3):427–43. [PubMed: 23420451]

Toth K, Magloczky Z. The vulnerability of calretinin-containing hippocampal interneurons to temporal lobe epilepsy. Front Neuroanat. 2014; 8:100. [PubMed: 25324731]

Unnithan AS, Choi HJ, Titler AM, Posimo JM, Leak RK. Rescue from a two hit, high-throughput model of neurodegeneration with N-acetyl cysteine. Neurochemistry international. 2012; 61(3): 356–368. [PubMed: 22691629]

Unnithan AS, Jiang Y, Rumble JL, Pulugulla SH, Posimo JM, Gleixner AM, Leak RK. N-acetyl cysteine prevents synergistic, severe toxicity from two hits of oxidative stress. Neurosci Lett. 2014; 560:71–6. [PubMed: 24361774]

Walker LC, Levine H 3rd, Mattson MP, Jucker M. Inducible proteopathies. Trends Neurosci. 2006; 29(8):438–43. [PubMed: 16806508]

Wang X, Wang W, Li L, Perry G, Lee HG, Zhu X. Oxidative stress and mitochondrial dysfunction in Alzheimer's disease. Biochim Biophys Acta. 2014; 1842(8):1240–7. [PubMed: 24189435]

Xia J, Miu J, Ding H, Wang X, Chen H, Wang J, Wu J, Zhao J, Huang H, Tian W. Changes of brain gray matter structure in Parkinson's disease patients with dementia. Neural Regen Res. 2013; 8(14):1276–85. [PubMed: 25206422]

Yong-Kee CJ, Warre R, Monnier PP, Lozano AM, Nash JE. Evidence for synergism between cell death mechanisms in a cellular model of neurodegeneration in Parkinson's disease. Neurotox Res. 2012; 22(4):355–64. [PubMed: 22528248]

Zhu X, Lee HG, Perry G, Smith MA. Alzheimer disease, the two-hit hypothesis: an update. Biochimica et biophysica acta. 2007; 1772(4):494–502. [PubMed: 17142016]

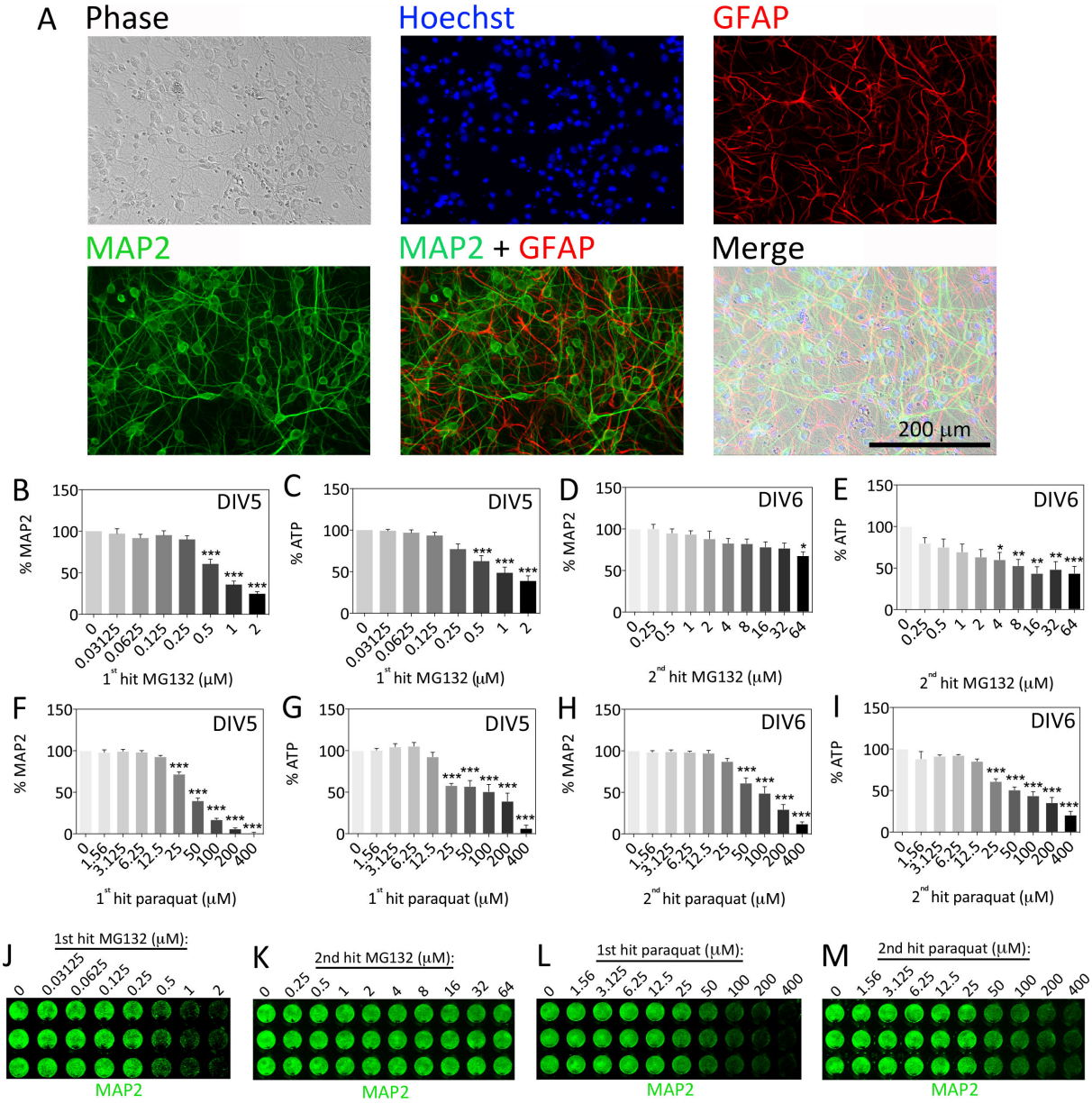

Figure 1. Characterization of primary hippocampal cultures and concentration-response curves

(A) Hippocampal cultures harvested from the postnatal rat brain were immunocytochemically stained on day *in vitro* 7 (DIV7) for the neuronal marker microtubule-associated protein 2 (MAP2, green) and the astrocyte marker glial fibrillary acidic protein (GFAP, red). Nuclei were stained blue with the Hoechst reagent. Photomicrographs were captured using a 20× objective on an epifluorescent microscope. **(B–M)** Primary hippocampal cultures were treated with MG132 or paraquat on DIV5 (1st hit) or DIV6 (2nd hit). Viability was assayed on DIV7 by **(B, D, F, H)** the In-Cell Western assay for MAP2 levels and **(C, E, G, I)** the Cell Titer Glo luminescent assay for ATP. Representative MAP2 In-Cell Western images are shown in panels **J–M**. Shown are the mean and SEM of 3–4 independent experiments, each performed in triplicate. *$p \leq 0.05$, **p

≤ 0.01, ***$p \leq 0.001$ versus 0 μM MG132 or paraquat, one-way ANOVA followed by Bonferroni *post hoc* correction.

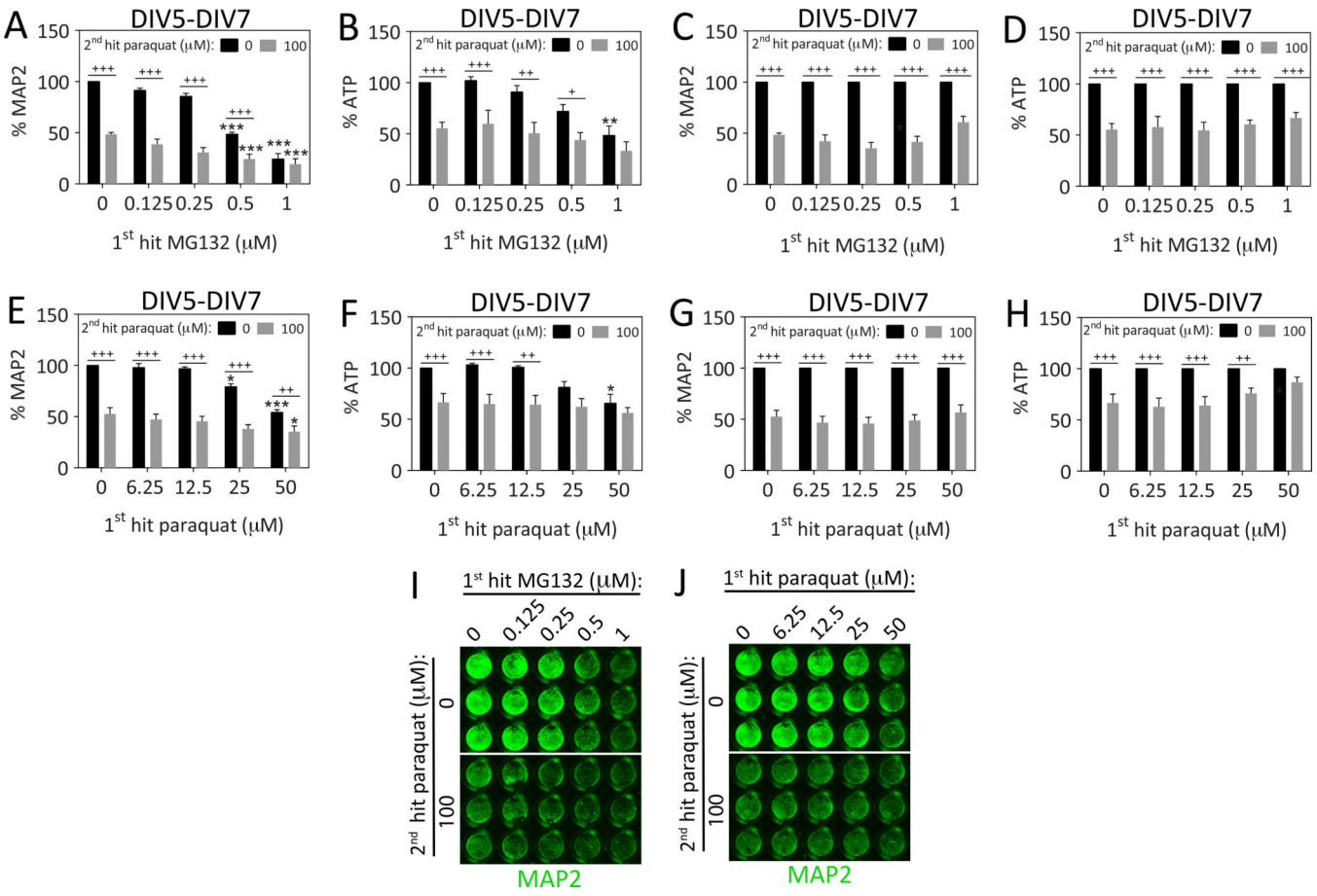

Figure 2. Dual hits of proteotoxic and oxidative stress are additive in their toxic effects 24h after the final insult

(A–D) Primary hippocampal cultures were treated on DIV5 with the 1st hit of MG132 and on DIV6 with the 2nd hit of paraquat. Viability was assayed 24h later on DIV7 by **(A)** the In-Cell Western assay for MAP2 levels and **(B)** the Cell Titer Glo luminescent assay for ATP. A representative MAP2 In-Cell Western image is shown in panel I. **(C–D)** In order to statistically evaluate the synergistic or additive nature of the dual hits, the data shown in panels A and B were also expressed as a function of the 0 μM paraquat 2nd hit group (*i.e.,* all gray bars were expressed as a percentage of the adjacent black bars). These latter measurements show more clearly that the 1st hit did not change the impact of the 2nd hit on DIV7. **(E–H)** Primary hippocampal cultures were treated on DIV5 with the 1st hit of paraquat followed by a 2nd hit of the same toxicant on DIV6. Viability was assayed on DIV7 by **(E, J)** the In-Cell Western assay for MAP2 levels and **(F)** the Cell Titer Glo luminescent assay for ATP. The same data were normalized to the 0 μM 2nd hit group in panels **G–H** and show that the 1st hit did not affect the toxicity of the 2nd hit according to the MAP2 assay and that the 1st paraquat hit blocked loss of ATP in response to the 2nd paraquat hit at high concentrations (50 μM). Shown are the mean and SEM of 3–6 independent experiments, each performed in triplicate. *$p \leq 0.05$, **$p \leq 0.01$, ***$p \leq 0.001$ versus 0 μM 1st hit; +$p \leq 0.05$, ++$p \leq 0.01$, +++$p \leq 0.001$ versus 0 μM 2nd hit; two-way ANOVA followed by Bonferroni *post hoc* correction.

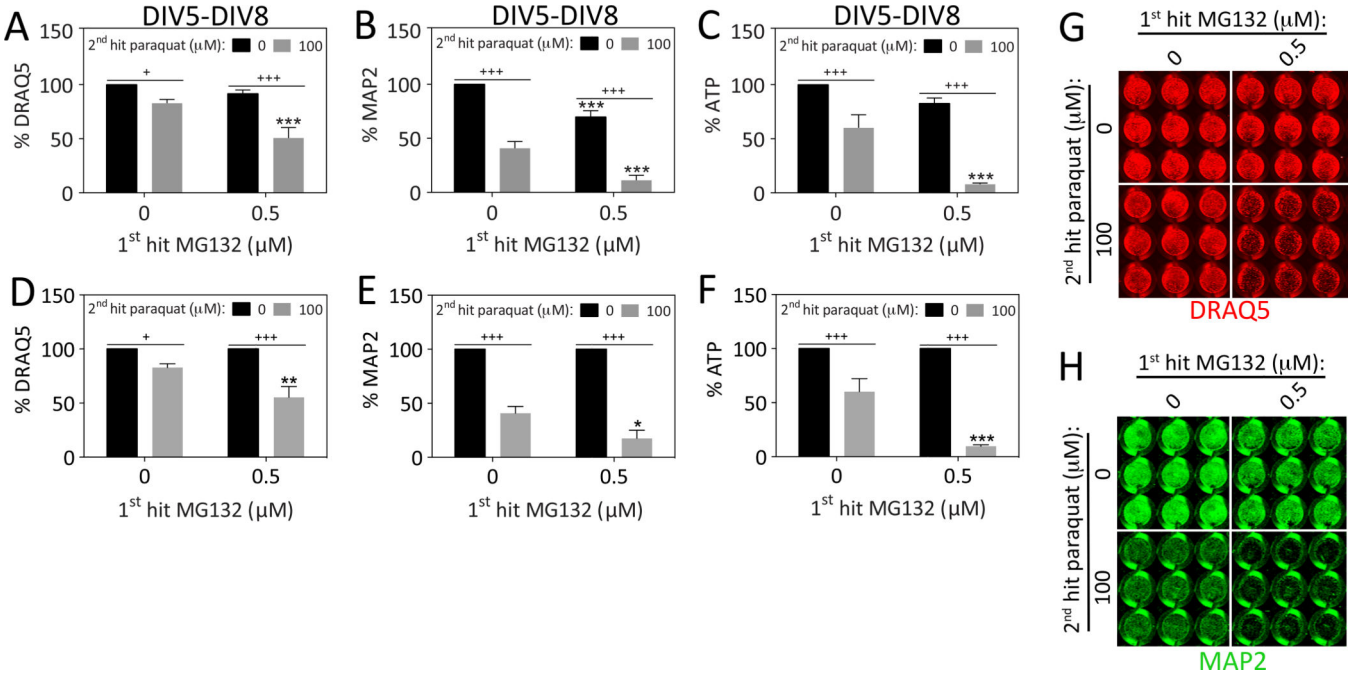

Figure 3. Dual hits of proteotoxic and oxidative stress are synergistic 48h after the final insult

Primary hippocampal cultures were treated on DIV5 with the 1st hit of MG132 and on DIV6 with the 2nd hit of paraquat. Viability was assayed 48h later on DIV8 by **(A)** the nuclear DRAQ5 stain, **(B)** the In-Cell Western assay for MAP2 levels, and **(C)** the Cell Titer Glo luminescent assay for ATP. Representative DRAQ5 and MAP2 images are shown in panels G and H. Panels **A–C** are shown as scatterplots in Supplemental Figure 3 (A–C) to show all individual data points. **(D–F)** The data shown in panels A–C were expressed as a function of the 0 μM paraquat 2nd hit group (*i.e.,* all gray bars were expressed as a percentage of the adjacent black bars). The latter measurements show statistically that the 1st hit significantly exacerbates the toxic impact of the 2nd hit on DIV8. Shown are the mean and SEM of 4 independent experiments, each performed in triplicate. *$p \leq 0.05$, **$p \leq 0.01$, ***$p \leq 0.001$ versus 0 μM 1st hit; +$p \leq 0.05$, ++$p \leq 0.01$, +++$p \leq 0.001$ versus 0 μM 2nd hit; two-way ANOVA followed by Bonferroni *post hoc* correction.

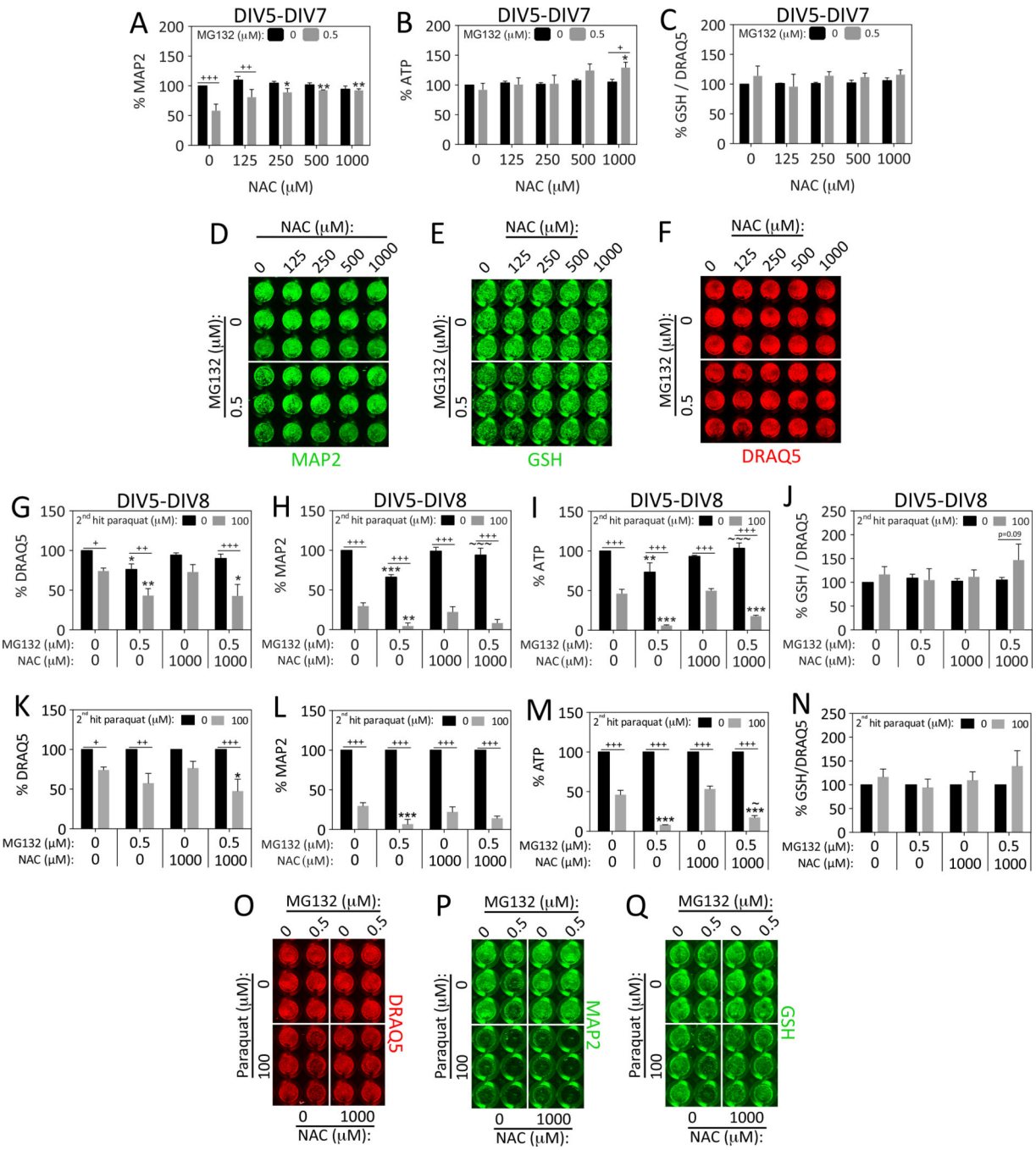

Figure 4. N-acetyl cysteine protects hippocampal neurons against proteotoxicity but not oxidative stress

Primary hippocampal cultures were treated on DIV5 with MG132 in the absence or presence of N-acetyl cysteine (NAC). Viability was assayed 48h later on DIV7 by **(A)** the In-Cell Western assay for MAP2 levels, and **(B)** the Cell Titer Glo luminescent assay for ATP. A representative MAP2 image is shown in panel **D. (C)** The same treatments as shown in panels A–B were repeated and glutathione (GSH) levels were measured by the In-Cell Western technique and expressed as a function of the nuclear DRAQ5 stain. Represented

images of glutathione and DRAQ5 staining are shown in panels **E** and **F**. For panels A–F: *$p \leq 0.05$, **$p \leq 0.01$, ***$p \leq 0.001$ versus 0 μM NAC; +$p \leq 0.05$, ++$p \leq 0.01$, +++$p \leq 0.001$ versus 0 μM MG132; two-way ANOVA followed by Bonferroni *post hoc* correction. **(G–Q)** Primary hippocampal cultures were treated on DIV5 with the 1st hit of MG132 and on DIV6 with the 2nd hit of paraquat in the absence or presence of NAC. Viability was assayed 48h later on DIV8 by **(G)** the nuclear stain DRAQ5, **(H)** the In-Cell Western assay for MAP2 levels, and **(I)** the Cell Titer Glo luminescent assay for ATP. Representative DRAQ5 and MAP2 images are shown in panels **O** and **P**. NAC mitigated MG132 but not paraquat toxicity and failed to protect against dual MG132/paraquat hits. Panels **G–I** are shown as scatterplots in Supplemental Figure 3 (D–F) to show all individual data points. **(J)** The same treatments as shown in panels G–I were repeated and glutathione (GSH) levels were measured by the In-Cell Western technique and expressed as a function of the nuclear DRAQ5 stain. A representative image of the glutathione In-Cell Western data is shown in panel Q. **(K–N)** Data shown in panels G–J were expressed as a percentage of the 0 μM 2nd hit group (each gray bar was expressed as a percentage of the adjacent black bar). Shown are the mean and SEM of 3–4 independent experiments, each performed in triplicate. For panels G–N: *$p \leq 0.05$, **$p \leq 0.01$, ***$p \leq 0.001$ versus 0 μM 1st MG132 hit; +$p \leq 0.05$, ++$p \leq 0.01$, +++$p \leq 0.001$ versus 0 μM 2nd paraquat hit; ~$p \leq 0.05$, ~~$p \leq 0.01$, ~~~$p \leq 0.001$ versus 0 μM NAC; three-way ANOVA followed by Bonferroni *post hoc* correction.

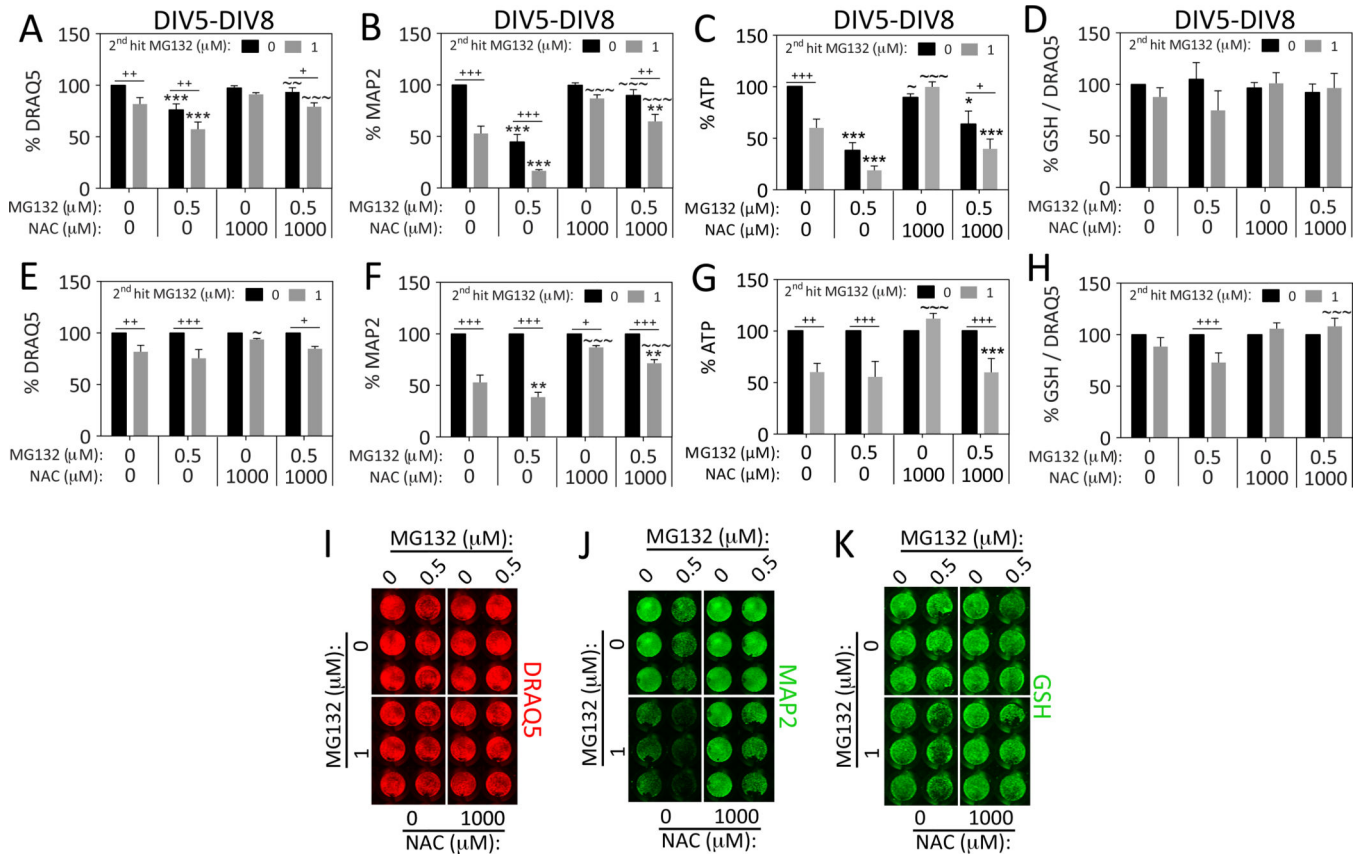

Figure 5. N-acetyl cysteine prevents loss of MAP2^{+} neuronal profiles after dual MG132/MG132 hits

Primary hippocampal cultures were treated on DIV5 with the 1st hit of MG132 and on DIV6 with the 2nd hit of MG132 in the absence or presence of N-acetyl cysteine (NAC). Viability was assayed 48h later on DIV8 by **(A)** the nuclear stain DRAQ5, **(B)** the In-Cell Western assay for MAP2 levels, and **(C)** the Cell Titer Glo luminescent assay for ATP. Representative DRAQ5 and MAP2 images are shown in panels **I** and **J**. Panels **A–C** are shown as scatterplots in Supplemental Figure 3 (G–I) to show all individual data points. **(D)** The same treatments as shown in panels A–C were repeated and glutathione (GSH) levels were measured by the In-Cell Western technique and expressed as a function of the nuclear DRAQ5 stain. A representative image of the glutathione In-Cell Western is shown in panel **K. (E–H)** Data in panels A–D are expressed as a function of the 0 μM 2nd hit group in order to statistically evaluate the effect of dual hits. NAC mitigated MG132 toxicity in response to single hits of MG132. The toxicity of dual MG132 hits was not ameliorated by NAC according to the DRAQ5 and ATP assays, but was mitigated by NAC in the MAP2 assay, which is specific for neuronal elements. The transformed data in panel **H** reveal that NAC prevents synergistic loss of GSH in response to dual MG132/MG132 hits. Shown are the mean and SEM of 3–5 independent experiments, each performed in triplicate. *$p \leq 0.05$, **$p \leq 0.01$, ***$p \leq 0.001$ versus 0 μM 1st hit; +$p \leq 0.05$, ++$p \leq 0.01$, +++$p \leq 0.001$ versus 0 μM 2nd hit; ~$p \leq 0.05$, ~~$p \leq 0.01$, ~~~$p \leq 0.001$ versus 0 μM NAC; three-way ANOVA followed by Bonferroni *post hoc* correction.

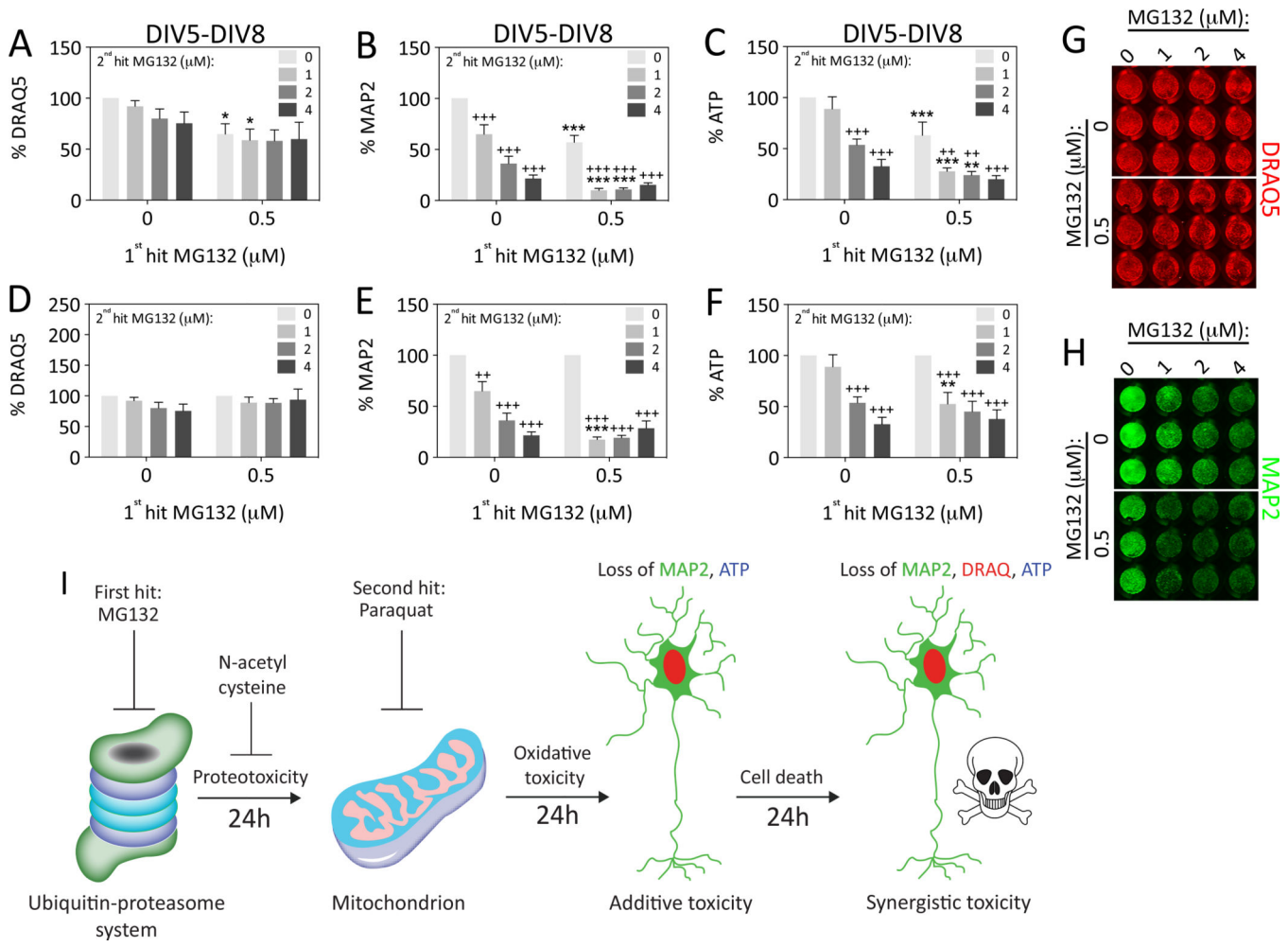

Figure 6. Impact of dual hits of MG132 on hippocampal neuron viability

Primary hippocampal cultures were treated on DIV5 with the 1st hit of MG132 and on DIV6 with a range of concentrations of MG132 as the 2nd hit. Viability was assayed 48h later on DIV8 by **(A)** the nuclear stain DRAQ5, **(B)** the In-Cell Western assay for MAP2 levels, and **(C)** the Cell Titer Glo luminescent assay for ATP. Representative DRAQ5 and MAP2 images are shown in panels **G** and **H**. Data are expressed as a function of the 0 μM 2nd hit group in panels **D–F** to statistically evaluate the effect of dual hits. The loss of viability in response to dual hits of MG132 was synergistic, but only at one concentration of the 2nd hit (1 μM) and not according to the DRAQ5 nuclear assay. Shown are the mean and SEM of 3–5 independent experiments, each performed in triplicate. *$p \leq 0.05$, **$p \leq 0.01$, ***$p \leq 0.001$ versus 0 μM 1st hit; +$p \leq 0.05$, ++$p \leq 0.01$, +++$p \leq 0.001$ versus 0 μM 2nd hit; two-way ANOVA followed by Bonferroni *post hoc* correction. **(I)** Summary schematic for the major findings in the present study. The images of the proteasome and mitochondrion are adapted from our previous drawings (Anne Stetler et al., 2013; Leak, 2014).